Electronic Supplementary Material (ESI) for ChemComm.

Supporting Information

Bio-inspired CO_2 Conversion by Iron Sulfide Catalysts under Sustainable Conditions

A. Roldan,[a] N. Hollingsworth,[a] A. Roffey,[a] H.U. Islam,[a,b] J.B.M. Goodall,[a] C.R.A. Catlow,[a] J.A. Darr,[a] W. Bras,[b] G. Sankar,[a] K.B. Holt,[a] G. Hogarth,[a] N.H. de Leeuw*[a]

[a] Department of Chemistry, University College London, 20 Gordon Street, London WC1H 0AJ, UK, n.h.deleeuw@ucl.ac.uk

[b] European Synchrotron Radiation Facility, Netherlands Organisation for Scientific Research NWO, F-38043 Grenoble, France

Contents

S1. General Information

S1.1 Experimental

S1.12 Synthesis of [Fe(S2CNiBu2)3]

$Fe(S_2CN^iBu_2)_3$ was synthesised according to an already existing literature report (White, A. H.; Roper, R.; Kokot, E.; Waterman, H.; Martin, R. L. *Australian Journal of Chemistry* **1964**, *17*, 294). An example of the synthesis method is given below.

$NaS_2NC^iBu_2$ (6.8210 g, 30 mmol) was dissolved into 60 mL water and added dropwise over 10 mins to a solution of $FeCl_3$ (1.6221 g, 10 mmol) dissolved in 50 mL of water, whereupon a black precipitate began to form. This mixture was vigorously stirred for 2 hrs, filtered, washed with water (3 x 30 mL) and evaporated to dryness. The black powder product was then dissolved in 100 mL of dichloromethane (DCM) and stirred with magnesium sulphate for 30 mins, after which the mixture was filtered and the filtrate dried *in vacuo*. Yield 5.5525 g, 83%. **Anal. Calc. for $C_{27}H_{54}N_3S_6Fe$:** C, 48.48; H, 8.14; N, 6.23. Found: C, 48.52; H, 8.26; N, 6.23. **MS:** *m/z* 669 [M^+], 464 [M^+ - $C_9H_{18}NS_2$]. **IR (ν_{max} cm^{-1}):** 1482 (s) [N=C], 992 (s), 1244 (s) [C=S], 1145 (s) [C_2N].

S1.13 Nano-particle synthesis

Carbon nano-particles donated by Johnson Matthey. EDX analysis showed the presence of only carbon and gold. Gold was due to the sample being mounted on a gold TEM grid.

S1.14 Pure Greigite

$Fe(S_2CN^iBu_2)_3$ (0.1 mmol, 0.0669 g) and $(Et_2NCS_2)_2$ (0.2 mmol, 0.0593 g) dissolved in 20 mL of oleylamine were placed in a round bottomed flask fitted with a condenser under a nitrogen atmosphere. The stirred solution was heated to 230^{o}C for 1 hour. The mixture was then allowed to cool slowly to room temperature, and washed with 3 x 100 mL methanol. The sample was then dispersed in chloroform, filtered and dried *in vacuo*.

S1.15 Greigite in a carbon matrix

$Fe(S_2CN^iBu_2)_3$ (0.1 mmol, 0.0669 g), $(Et_2NCS_2)_2$ (0.2 mmol, 0.0593 g) and C_{nano} (8.2 mmol,0.0987) were stirred in 20 mL of oleylamine, in a round bottomed flask fitted with a condenser under a nitrogen atmosphere. The solution was heated to 230^{o}C with stirring and held there for 1 hour. The mixture was then cooled slowly to room temperature, and washed with 3 x 100 mL methanol. The sample was then dispersed in chloroform and dried *in vacuo*.

S1.2 Catalyst testing

S1.21 Set up

H-cell setup (Figure S1) the working electrode is a carbon rod, 3mm diameter, 55mm length. The reference electrode is $Ag/AgCl_2$ in saturated KCl. The counter electrode is a 0.5mm diameter 250mm length Pt wire coiled to fit within the cell. The H-cell membrane is 25.4mm dialysis tubing supplied from Scientific Laboratory supplies (TUB2014). A 0.2 M PBS buffer (pH 6.5) is used unless otherwise stated. The H-

cell is thoroughly washed in several portions of deionised water (Milli-Q 18.2MΩcm at 25°C) prior to use.

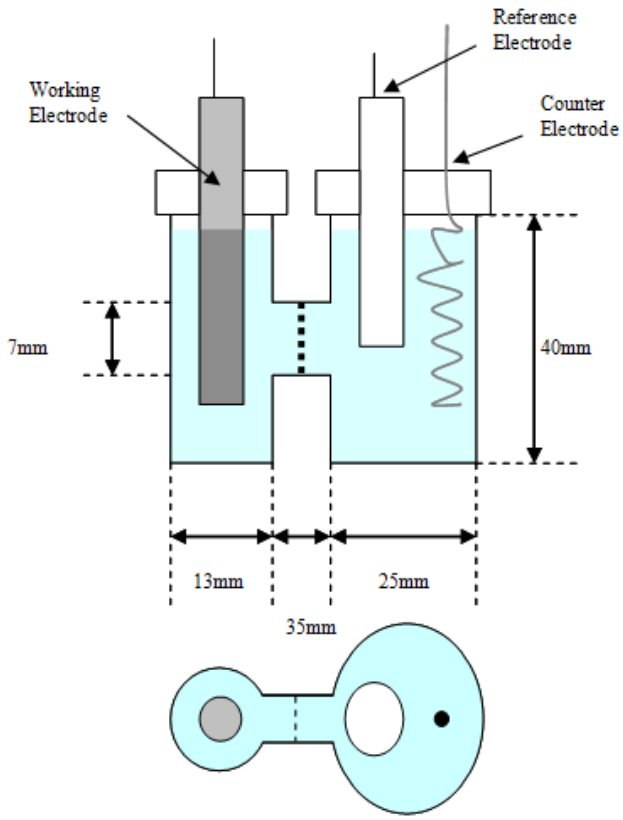

Figure S1 – Electro reduction H-cell

S1.22 Electrode preparation

A carbon rod electrode is washed three times with deionised water (DI) then placed in a vial containing deionised water (DI) water and cleaned by sonication. The electrode is then washed three additional times with DI water. Any additional water is removed from the electrode with compressed air. The electrode is then dried *in vacuo* for 1 hr.

The electrode is weighed and the nano-particles (Greigite in a nano-carbon matrix), suspended in dichloromethane, are evenly drop-coated onto the carbon rod electrode (Figure S2). 35 mm of the electrode was coated for each electrode, representing a electrode surface area of 688 mm^2. The electrode is placed under vacuum for 1 hr to remove any remaining dichloromethane and weighed to determine the amount of catalyst on the electrode.

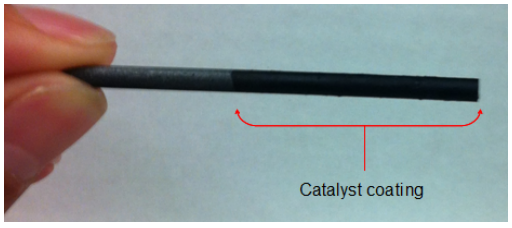

Figure S2- an example of a coated electrode

S1.23 Catalyst cleaning method

0.2 M PBS buffer is degassed with Ar (15 mins) and a ^{1}H NMR spectra is taken to ensure no contaminants are present (Figure S3). The only peak acceptable is that of water.

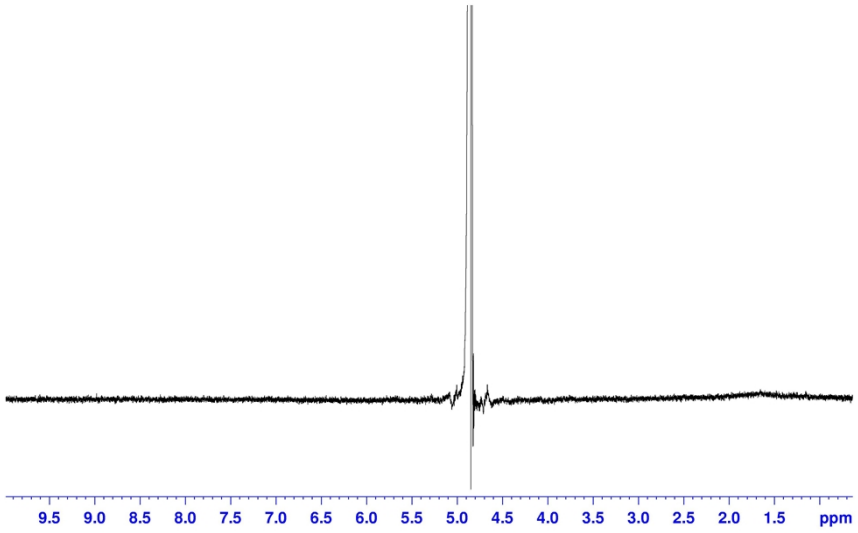

Figure S3- no contaminants present

The clean buffer is placed in the clean H-cell. The electrode is sealed within the H-cell and connected to the potentiostat. A scanning potential is applied to the sample from 0 to -1 V at 1 mVs^{-1} for at least 32 scans.

The electrode is removed and stored in a sample vial under Ar. A ^{1}H NMR spectrum is taken of the electrolyte in the working electrode compartment. This is the cleaning stage so you should expect to see some organics.

The H-cell is then thoroughly cleaned 4 times with DI water. Fresh 0.2 M PBS buffer is then degassed with Ar (15 mins) and a ^{1}H NMR taken to ensure no contaminants are present before the electrolyte is placed in the H-cell.

The electrode is sealed within the H-cell and connected to the potentiostat. A further 32 scans are performed.

The electrode is removed and stored in a sample vial under Ar. ^{1}H NMR is taken of the electrolyte in the working electrode compartment. The ^{1}H NMR spectra is now comparable to Figure 8. The justification for electrode cleaning is due to IR evidence suggesting greigite nano-particles absorb CO_2 from the atmosphere on standing. As such the electrode is cleaned in order to start from a clean surface.

S1.24 Catalyst testing procedure

The H-cell is thoroughly cleaned 4 times with DI water. 0.2 M PBS buffer is degassed with Ar (15 mins), saturated with CO_2 (15 mins) and placed in the H-cell after a ^{1}H-NMR spectrum is recorded to ensure no contaminants are present.

The electrode is sealed within the H-cell and connected to the potentiostat and scanned from 0 to -1V at 1 mVs^{-1}.

The experiment is then stopped at intervals. The number of scans recorded and 0.36ml of electrolyte removed from the working electrode compartment. This sample is then analysed by quantitative ^1H NMR analysis. Fresh 0.2 M PBS buffer is then degassed with Ar (15 mins), saturated with CO_2 (15 mins) and checked by a ^1H NMR spectrum to ensure that no contaminants are present. 0.36ml of this solution is then added to the working electrode compartment in order to maintain a constant volume of solution. The potentiostat is then restarted; the process of sampling is then repeated.

S1.3 Controls

To test that organics detected are from reduction on the greigite surface several controls have been performed.

S1.31 Control 1 – no greigite

Preparation of carbon electrode: Carbon nanoparticles are stirred in oleylamine (20ml) under N_2 and the mixture heated to 240°C for 1hr. This is analogous to the processing conditions the carbon nano-particles undergo whilst being loaded with greigite. The carbon nano-particles are washed three times with methanol and suspended in dichloromethane.

The carbon rod is then coated in an analogous way to S1.22, the particles are cleaned following S1.23 and tested using the procedure outlined in S1.24.

Qualitative ^1H NMR analysis (Figure S4) shows **no** presence of product.

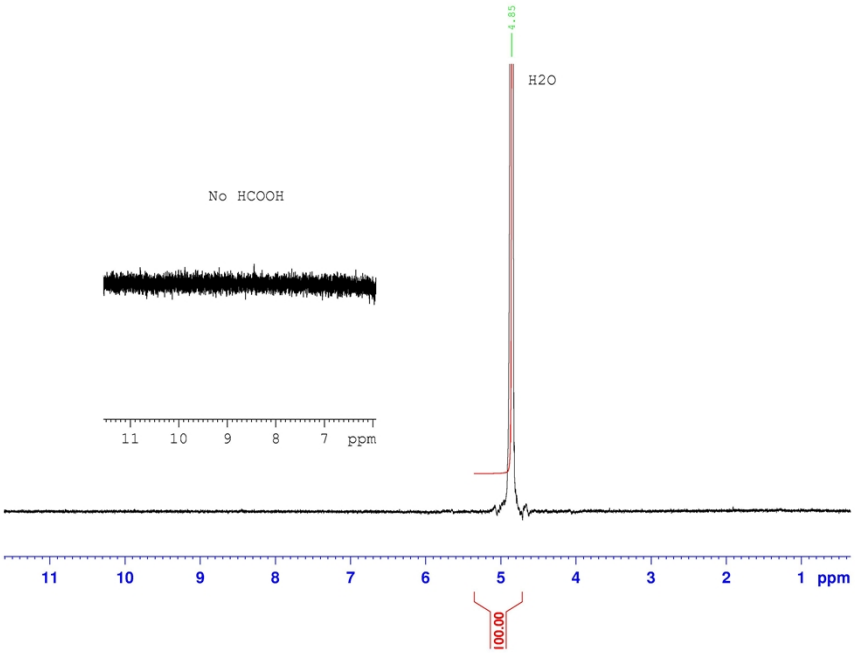

Figure S4 – Control 1, ^1H NMR

The results from the control strongly suggest greigite in a nano carbon matrix under a scanning potential from 0 to -1 V is able to reduce CO_2 to formic acid.

S1.32 Control 2 - no CO_2

Following procedure 3.21, 3.22 and modifying 3.23 to exclude saturating the electrolyte with CO_2 yields no detectable product.

S1.4 Quantitative ^{1}H NMR analytical protocol

Liquid phase products were analysed by ^{1}H NMR spectroscopy. NMR spectra were recorded on a Bruker Advance III 600 MHz NMR, equipped with cryoprobe and quantified with a 1% $Me_4Si/CDCl_3$ internal standard sealed in a glass tube, which was calibrated against primary standards. Typically, 0.36ml of sample and 0.04ml D_2O were placed in an NMR tube along with the internal standard. A solvent suppression was run in order to minimise the signal arising from the solvent and chemical shifts were reported in parts per million relative to Me_4Si. The ^{1}H NMR experiment was repeated 3 times for each sample to account for instrumental error.

S1.41 Insert preparation

A coaxial insert for external lock & reference solvents (Sigma-Aldrich supplier, NI5CCI-B, tube-5mm, OD-2mm, length-50mm, capacity-100µL, sample capacity-490 µL) is filled with $CDCl_3$ containing 1% TMS (supplied from Sigma-Aldrich) and sealed by the glass blower.

S1.42 Insert calibration

Several solutions of 0.2 M PBS buffer are prepared containing 0.15, 0.1, 0.05, 0.025, 0.015 µmol/ml of formic acid. The samples are then analysed using the ^{1}H NMR quantitative procedure described earlier. The peak at 0ppm is TMS, which should be integrated and fixed at 10000. The peak at 8.4ppm is *H*COOH, which should be integrated. Note; NMR spectra for each calibration point should be repeated at least three times and integrals averaged to account for instrumental error.

Performing the same analysis on each concentration allows you to plot a calibration curve from the averages of the integrated spectra (Figure S5).

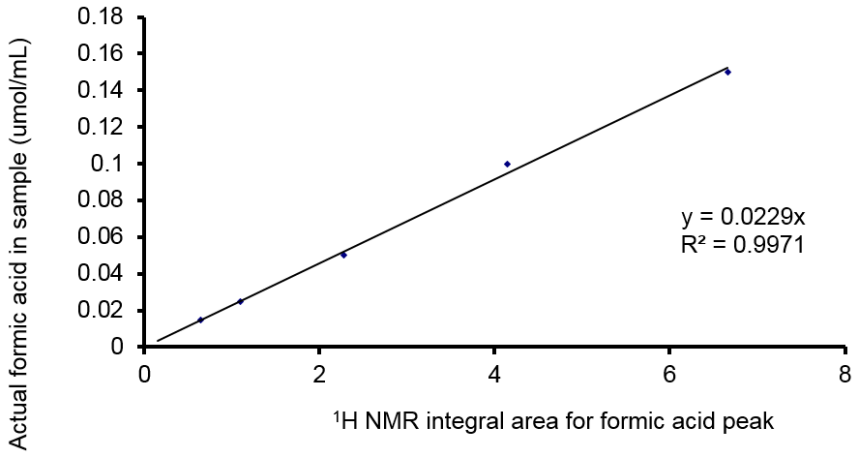

Figure S5 - Insert A formic acid calibration plot.

The gradient of the calibration plot is 0.0229, which is the calibration factor. For future analysis of unknown concentration samples, setting the TMS peak at 0ppm to an integration of 10000 before multiplying the integration of the formic acid proton by the calibration factor, will give the formic acid concentration in µmol/ml.

The calibration for the insert has been cross-checked with methanol. Several concentrations of MeOH in PBS were made up and ^{1}H NMR spectra taken, giving a calibration factor in close agreement, at 0.0219 per proton showing an error of less than 5%.

S1.43 Product Peak Positions

In order to identify the products of CO_2 reduction, several likely products have been placed in PBS buffer and ^{1}H NMR spectra taken (Figure S6)

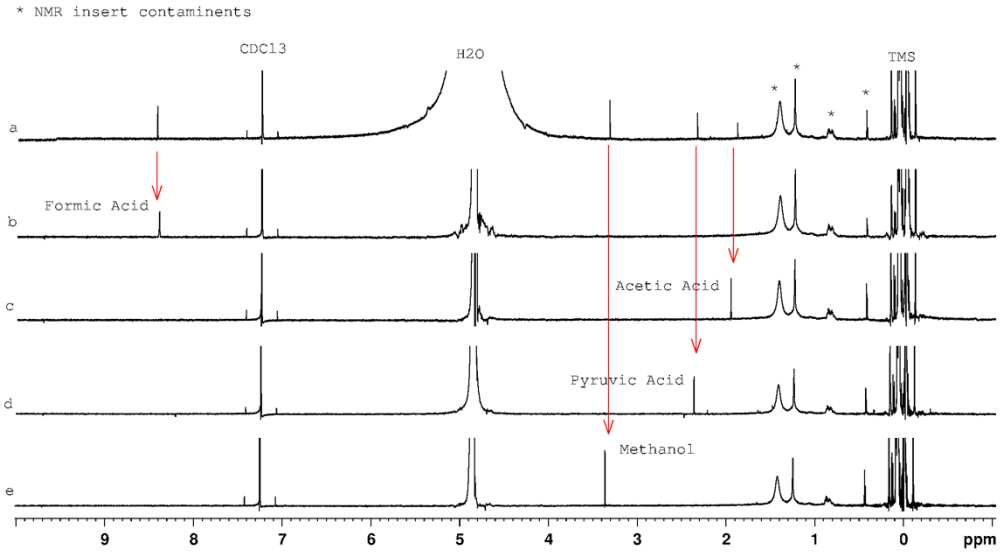

Figure S6 – peak positions of bought samples b-e in PBS buffer, a represents a CO_2 reduction sample at pH 6.5.

The products of CO_2 reduction were identified as formic acid (8.44 ppm), methanol (3.34 ppm), pyruvic acid (2.36 ppm) and acetic acid (1.91 ppm). The peaks positions were in good agreement with commercially available samples of formic acid (8.45 ppm), methanol (3.36 ppm), pyruvic acid (2.37 ppm) and acetic acid (1.97 ppm) recorded in 0.2M PBS using the same protocol.

S1.5 Computational Methods

S1.51 DFT calculations

We have carried out a systematic DFT-D2 study of the Fe_3S_4 surfaces, as well as reactants, intermediates and products related to the CO_2 transformation toward organic molecules. All calculations were performed using the VASP code,[1] where the ion–electron interactions were represented by projector-augmented wave (PAW) method[2] and the exchange-correlation by the generalized gradient approximation (GGA) with the Perdew–Wang 91 functional[3] and the spin interpolation formula of Vosko *et al*.[4] All the calculations include the long-range dispersion correction approach by Grimme,[5] which is an improvement when considering large polarisable atoms.[6] We have used the global scaling factor parameter optimized for PBE, (s_6=0.75). The Kohn-Sham valence states were expanded in a plane-waves basis set with a cut off at 600 eV for the kinetic energy.[7] This high value for the cut off energy ensured that no Pulay stresses occurred within the cell during relaxations. The initial magnetic moment was described by high-spin distribution in both types of Fe, octahedral (B) and tetrahedral (A), by a ferrimagnetic orientation.[8] Calculations were carried out described by a Monkhorst-Pack grid 4x4x1 for Fe_3S_4(001) and 5x5x1 K-points for Fe_3S_4(111) ensuring the electronic and ionic convergence.[9] We used the Hubbard approximation (U) for an accurate treatment of the electron correlation in the localized *d*-Fe orbital.[10] It improves the description of localized states in this type of systems, where standard LDA and GGA functionals fail.[11] A problem with this Hubbard approximation is the rather empirical character of the U parameter choice, a feature which also appears when using hybrid functionals, since the amount of Fock exchange is system dependent.[11-12] Therefore, we followed the approach used by Devey *et al*.[13] to obtain the U parameter (U= 1 eV) whose reliability has been tested for catalytic processes.[14] The geometries of all stationary points were found with the conjugate-gradient algorithm and considered converged when the force on each ion dropped below 0.03 eV/Å and the energy threshold defining self-consistency of the electron density was set to 10^{-5} eV. In order to improve the convergence of the Brillouin-zone integrations, the partial occupancies were determined using the tetrahedron method with Blöchl corrections, with a set smearing width for all calculations of 0.02 eV. These smearing techniques can be considered as a form of finite-temperature DFT, where the varied quantity is the electronic free energy.[7]

Besides the steady states defining the stages along the reaction mechanism, there is one saddle point linking both systems (if it is an elementary single step). These saddle points are the reaction transition states (TS) and they determine the kinetics of the process. We look for these particular points by means of either the dimer method[15] or Climbing Image Nudge Elastic Band (CI-NEB).[16] The CI-NEB links reactants and products by a set of images distributed among the reaction coordinate, whereas the dimer method searches the TS by giving an initial atomic velocity towards the particular final state (product(s)). From an initial configuration, we generate the initial velocities by making two equal and opposite small finite-difference displacements in the coordinates of the reactant molecule. Then, it finds a nearby saddle point by rotation and translation steps implemented with a conjugate gradient optimizer. The identified saddle point (TS) is further confirmed by a vibrational frequency calculation, in which only one imaginary (negative) frequency is obtained corresponding with the reaction coordinate. Afterwards, the dimer images are relaxed

to the neighbouring local minima. In a successful search, one of the images will minimize to the initial state and the other will give the final state.

S1.6 References

[1] aG. Kresse, J. Hafner, *Phys. Rev. B* **1993**, *47*, 558; bG. Kresse, J. Furthmüller, *Comput. Mat. Sci.* **1996**, *6*, 15.

[2] G. Kresse, D. Joubert, *Phys. Rev. B* **1999**, *59*, 1758.

[3] J. P. Perdew, J. A. Chevary, S. H. Vosko, K. A. Jackson, M. R. Pederson, D. J. Singh, C. Fiolhais, *Phys. Rev. B* **1992**, *46*, 6671.

[4] S. H. Vosko, L. Wilk, M. Nusair, *Can. J. Phys.* **1980**, *58*, 1200-1211.

[5] S. Grimme, *J. Comput. Chem.* **2006**, *27*, 1787-1799.

[6] aS. Irrera, A. Roldan, G. Portalone, N. H. De Leeuw, *The Journal of Physical Chemistry C* **2013**, *117*, 3949-3957; bN. Y. Dzade, A. Roldan, N. H. de Leeuw, *The Journal of Chemical Physics* **2013**, *139*, 124708-124708; cS. S. Tafreshi, A. Roldan, N. Y. Dzade, N. H. de Leeuw, *Surf. Sci.* **2014**, *622*, 1-8; dS. Haider, A. Roldan, N. H. de Leeuw, *The Journal of Physical Chemistry C* **2013**.

[7] N. D. Mermin, *Physical Review* **1965**, *137*, 1441-&.

[8] A. Roldan, D. Santos-Carballal, N. H. de Leeuw, *The Journal of Chemical Physics* **2013**, *138*, 204712-204716.

[9] H. J. Monkhorst, J. D. Pack, *Phys. Rev. B* **1976**, *13*, 5188-5192.

[10] aV. I. Anisimov, M. A. Korotin, J. Zaanen, O. K. Andersen, *Phys. Rev. Lett.* **1992**, *68*, 345-348; bS. L. Dudarev, G. A. Botton, S. Y. Savrasov, C. J. Humphreys, A. P. Sutton, *Phys. Rev. B* **1998**, *57*, 1505-1509.

[11] I. D. R. Moreira, F. Illas, R. L. Martin, *Phys. Rev. B* **2002**, *65*.

[12] aI. Ciofini, F. Illas, C. Adamo, *J. Chem. Phys.* **2004**, *120*, 3811-3816; bF. Illas, R. L. Martin, *J. Chem. Phys.* **1998**, *108*, 2519-2527; cD. Munoz, N. M. Harrison, F. Illas, *Phys. Rev. B* **2004**, *69*.

[13] A. J. Devey, R. Grau-Crespo, N. H. de Leeuw, *Phys. Rev. B* **2009**, *79*, 195126-195133.

[14] J. Wang, S.-H. Cao, W. Wu, G.-m. Zhao, *arXiv:1012.2364v1* **2011**.

[15] aG. Henkelman, H. Jonsson, *J. Chem. Phys.* **1999**, *111*, 7010-7022; bA. Heyden, A. T. Bell, F. J. Keil, *J. Chem. Phys.* **2005**, *123*.

[16] aG. Henkelman, H. Jonsson, *J. Chem. Phys.* **2000**, *113*, 9978-9985; bG. Henkelman, B. P. Uberuaga, H. Jonsson, *J. Chem. Phys.* **2000**, *113*, 9901-9904.

[17] G. W. Watson, E. T. Kelsey, N. H. deLeeuw, D. J. Harris, S. C. Parker, *Journal of the Chemical Society-Faraday Transactions* **1996**, *92*, 433-438.

[18] P. W. Tasker, *J Phys C Solid State* **1979**, *12*, 4977-4984.

S2. Supplementary Equations

S2.1 Energy profile

The binding energies of the adsorbents on the Fe_3S_4 surfaces were calculated according to **equation S1** for molecules interacting with the surface (E_B).

$$E_B = E_{Adsorbants:Fe_3S_4} - \left(E_{Fe_3S_4} + \sum_{i=1}^{Adsorbants} E_i \right) \qquad \textbf{(S1)}$$

where $E_{Adsorbants:Fe3S4}$ is the total energy of the system containing the Fe_3S_4 slab and a molecule(s) interacting with it, E_{Fe3S4} is the energy of the naked Fe_3S_4 slab and E_i is the energy of the isolated molecule in vacuum.

The zero value for the energy on the profile is for a system consisting of H_2CO_3 and H_2O in the gas phase plus the bare (111) surface, where H_2O is taken as the source of adsorbed H atoms, instead of H_2 or protons, leading to co-adsorbed OH on the surface after dissociation of the water molecule. The adsorbed OH is assumed to play no further role in the reaction. Furthermore, the model considers low H ad-atom coverage, where the diffusion of surface-adsorbed H atoms is non-rate limiting. The energy barrier (ΔE^{TS}) of a certain process is the energy required to surmount the potential barrier characteristic of a transition state (TS). We defined this barrier energy as the difference between initial state and transition state for the forward process as **equation S2**.

$$\Delta E^{TS} = E_{TS} - E_{Initial} \qquad \textbf{(S2)}$$

We also defined the reaction energy (E_R) as the total energy difference between the final state (products) and the initial state (reactants) in **equation S3**.

$$E_R = E_{Final} - E_{Initial} \qquad \textbf{(S3)}$$

S3. Supplementary Data

S3.1 TEM

Performed on a JEOL 2100 TEM

S3.1.1 Pure Greigite

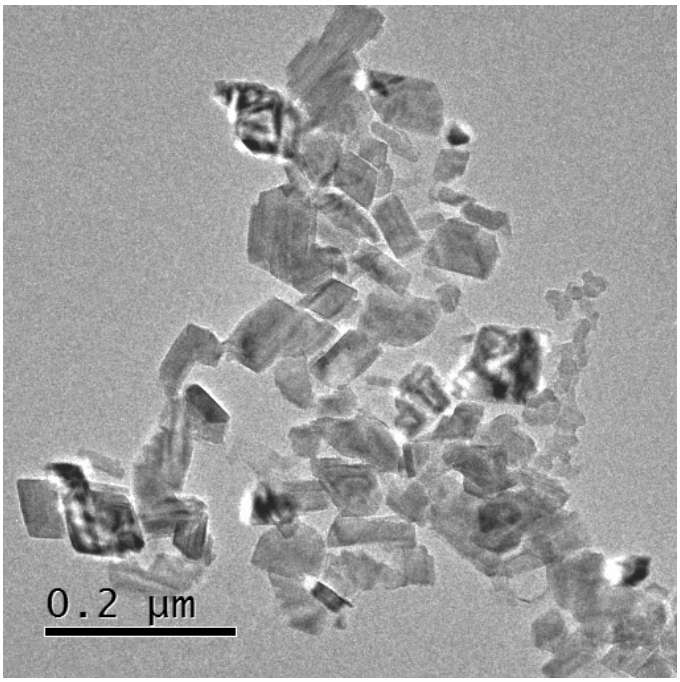

Figure S7 - TEM representing greigite particles

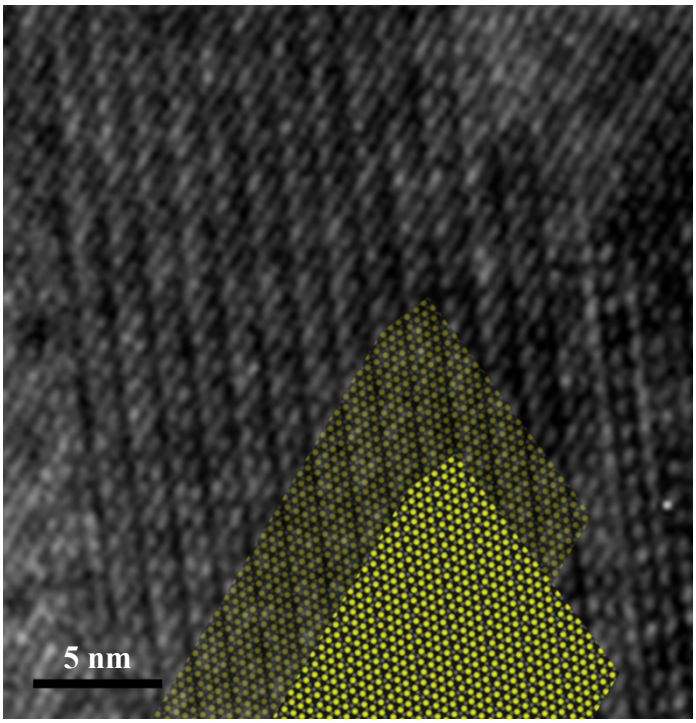

Figure S8 - HRTEM representing a particle edge, coloured area represents the top atomic layer in full intensity and 50 % transparent allowing a direct comparison with the actual surface structure.

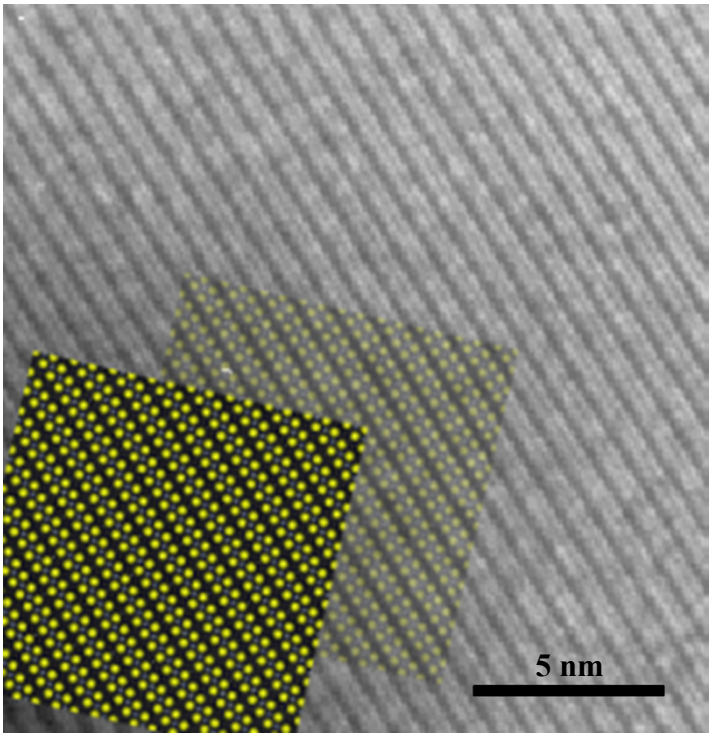

Figure S9 – HRTEM representing a particle surface, coloured squares represent the surface top atomic layer in full intensity and 50 % transparent allowing a direct comparison with the actual surface.

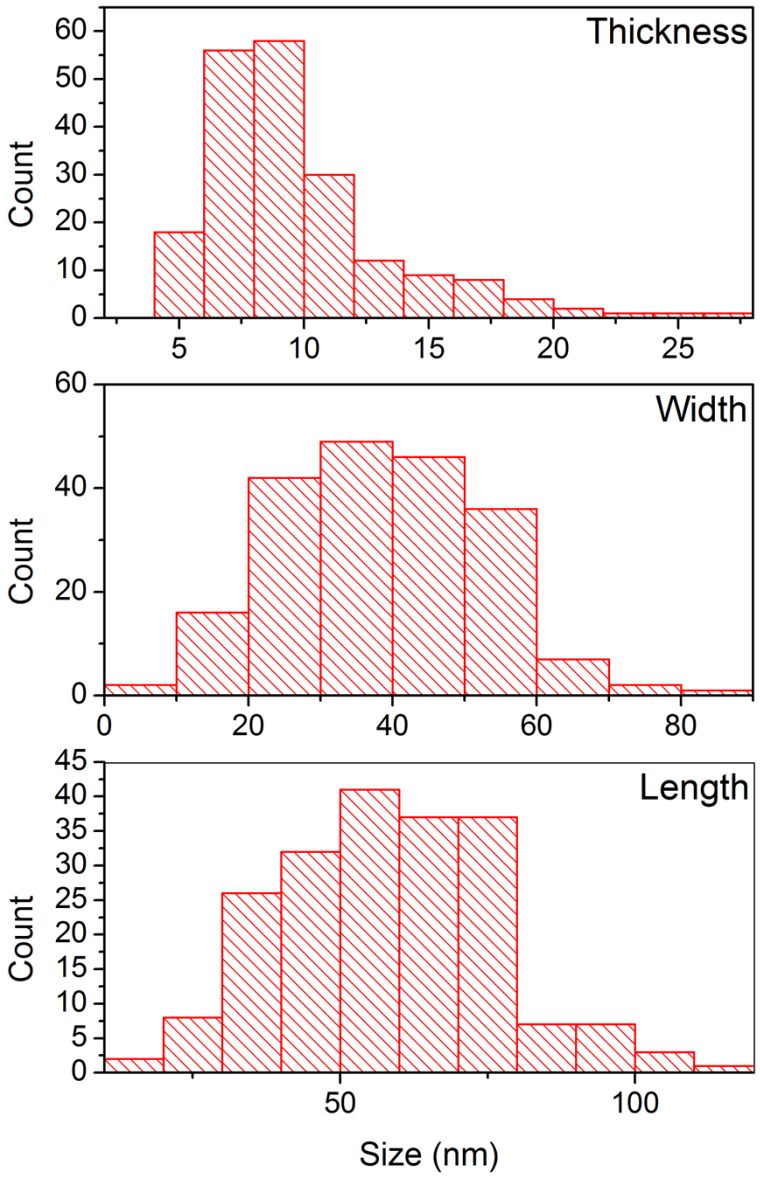

Figure S10 - Histograms of sheet dimensions

Average particle size: 58.02 x 38.43 x 9.72 nm. HRTEM shows the faces to be [1, 0, 0] and the edges to be [1, 1, 1].

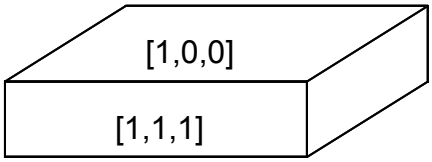

Figure S11 – Schematic representation of particle morphology.

S3.1.2 Greigite within a carbon matrix

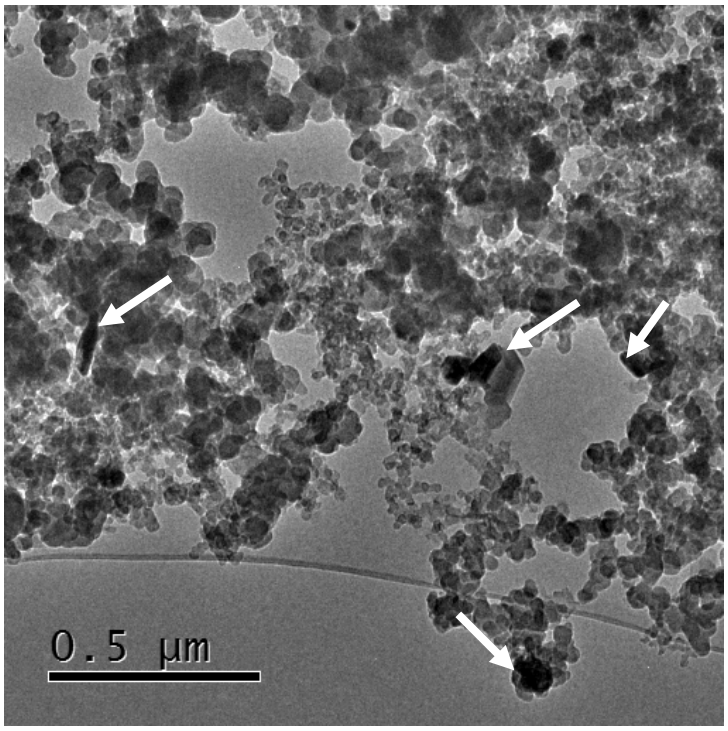

Figure S12 – TEM of Greigite in a carbon matrix, several greigite nano-sheets indicated by white arrows

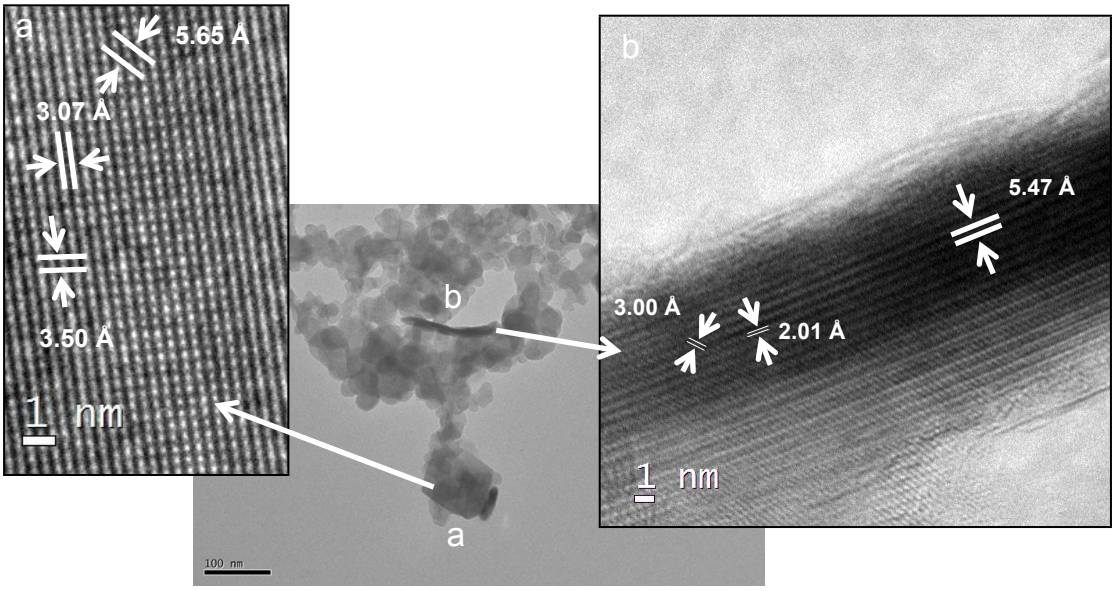

Figure S13 – Centre, TEM image showing greigite face (a) and edge (b) within a matrix of C_{nano}, right and left displays are corresponding HRTEM images.

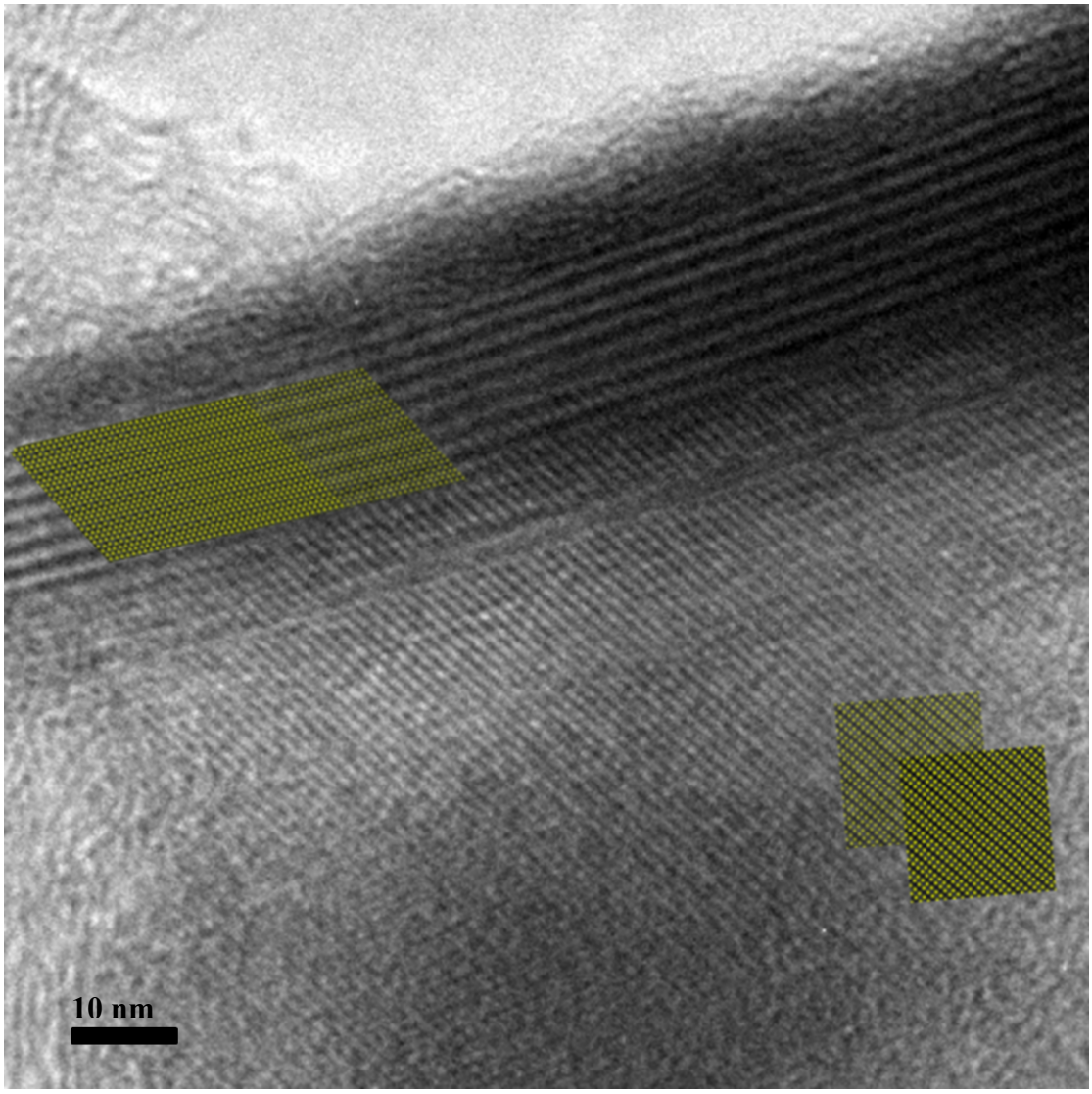

Figure S14 - TEM showing edge and face of greigite nano in carbon matrix, coloured areas represent the surface top atomic layer in full intensity and 50 % transparent allowing a direct comparison with the actual surface.

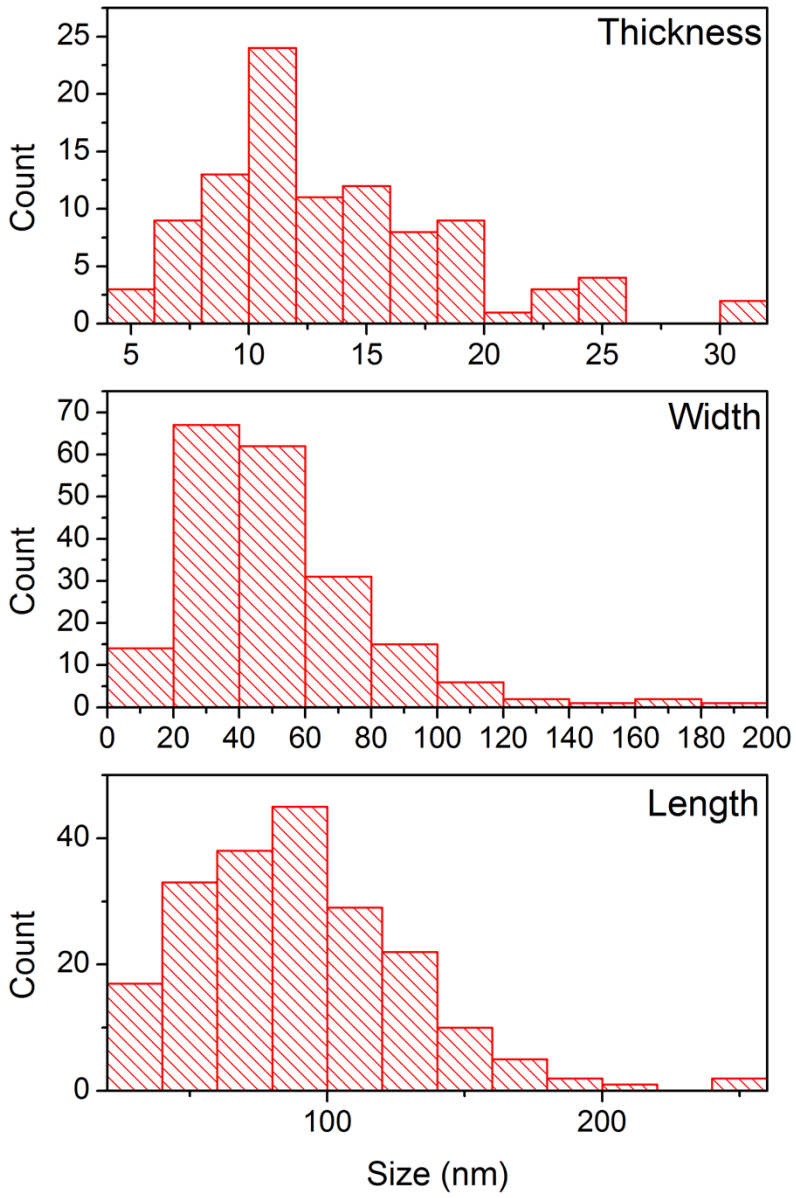

Figure S14 - Histograms of sheet dimensions

Average particle size: 110.59 x 66.44 x 17.89 nm. HRTEM shows the surface to be [1, 0, 0] and the edges to be [1, 1, 1].

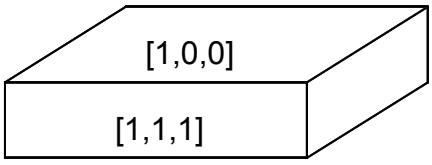

S3.2 XRD

Samples were analysed on a Brucker D4 diffractometer using a Cu source; the diffractometer was fitted with a post diffraction monochromator to reduce the effect of Fe florescence.

XRD data confirms the presence of a thiospinel with space group Fd3m. Figure S15 shows a phase match with as reported greigite (ICSD card no: 01-089-1999 16-713).

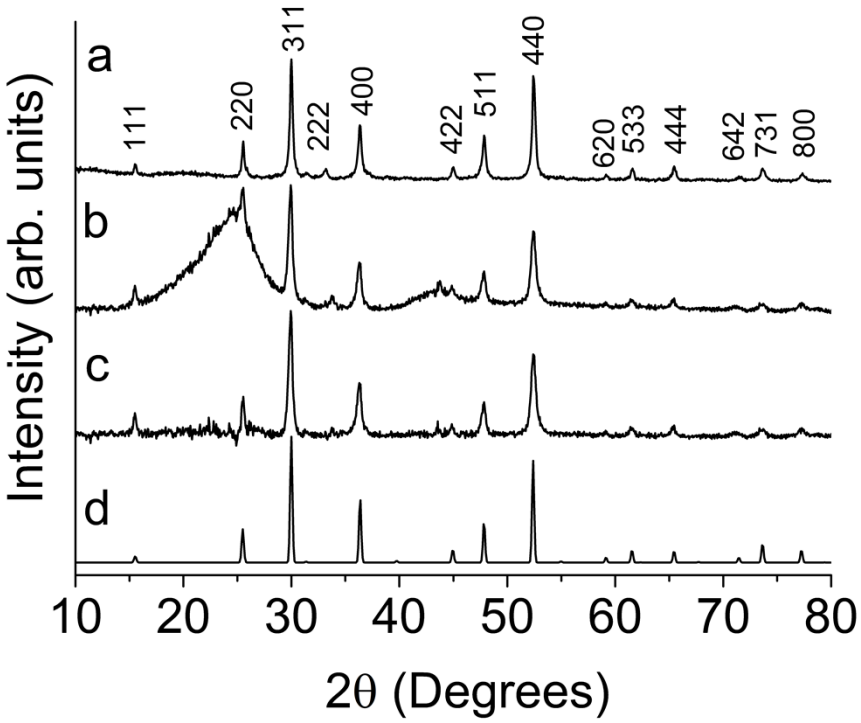

Figure S15 - Powder XRD of a) pure nano greigite b) greigite in a carbon matrix c) b minus background arising from amorphous carbon nano d) greigite PDF card 01-089-1999 16-713

S3.3 EXAFS

EXAS data of carbon loaded greigite were acquired in fluorescence on the Dutch-Belgian beamline BM26A at the ESRF (S. Nikitenko, A. M. Beale, A. M. J. van der Eerden, S. D. M. Jacques, O. Leynaud, M. G. O'Brien, D. Detollenaere, R. Kaptein, B. M. Weckhuysen and W. Bras, *J. Synchrotron Rad* **15**, 632-640 (2008)

The data were processed on Horea Athena (B. Ravel and M. Newville, *J. Synchrotron Rad.* **12**, 537-541 (2005)) and EXAFS modelling of the 1st shell was performed on Excurve98 (Binsted N, EXCURV98: CCLRC Daresbury Laboratory computer program (1998)). Coordination remained fixed at calculated values while bond distance and Debye-Waller factor were varied.

EXAFS modelling reveals the existence of three distinct bond distances shown in Table 1. Distances correspond to average tetrahedral Fe-S, octahedral surface Fe-S, and octahedral bulk Fe-S. The EXAFS derived distances are in good agreement with the calculated distances.

Table S1 - List of fitting parameters derived from EXAFS analysis of greigite in a carbon matrix

Scatter	*N*	R_{THEORY} (Å)	R_{EXAFS} (Å)	σ^2 (Å^2)	*F*
S	1.46	2.22	2.19 ± 0.01	0.006	
S	2.14	2.33	2.36 ± 0.01	0.006	40
S	1.60	2.46	2.44 ± 0.02	0.013	

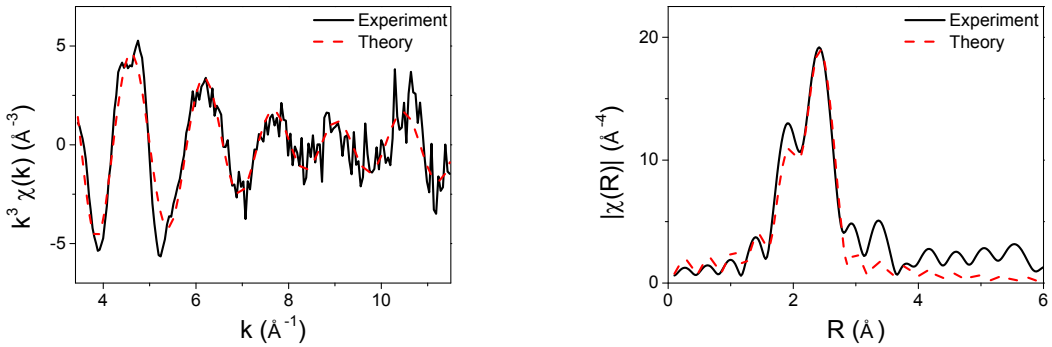

Figure S16 – Experimental and theoretical fits for, left, EXAFS and right, Fourier transform of greigite in a carbon matrix.

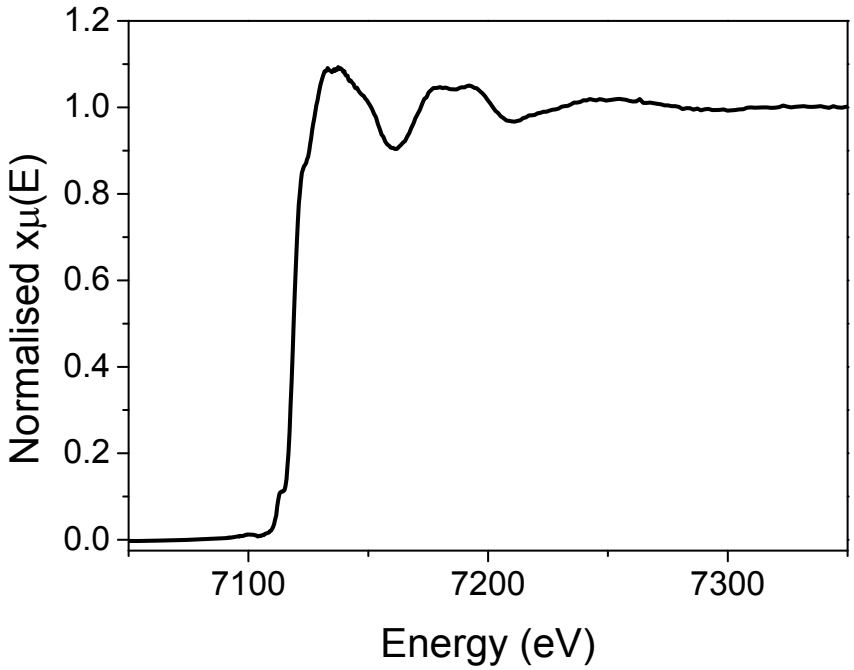

Figure S17- XAS of carbon coated greigite

S3.4 Carbon loading

Micro-analysis performed at the UCL in-house service by Jill Maxwell. Weight % C, 90.16; H, 1.51; N, 0.56;

Assuming the 0.56 N found is due to oleylamine capping agent ($C_{18}H_{37}N$, C- 80.82%, H- 13.94%, N- 5.24%) then we should expect to see 1.48 H from the hydrogen atoms

in OA, we see 1.51 which is in close agreement. The remainder is assumed to be Fe_3S_4 resulting in a 7.77 % loading of Fe_3S_4.

S3.5 Catalyst Testing Results

Electro-catalytic reduction of 10mg of greigite in a carbon matrix. For each new pH a new carbon rod electrode with fresh catalyst is added. The catalyst within a carbon matrix is from the same analysed batch. The following ^{1}H NMR spectra are after the clean stage.

S3.5.1 ^{1}H NMR Spectra

pH 4.5

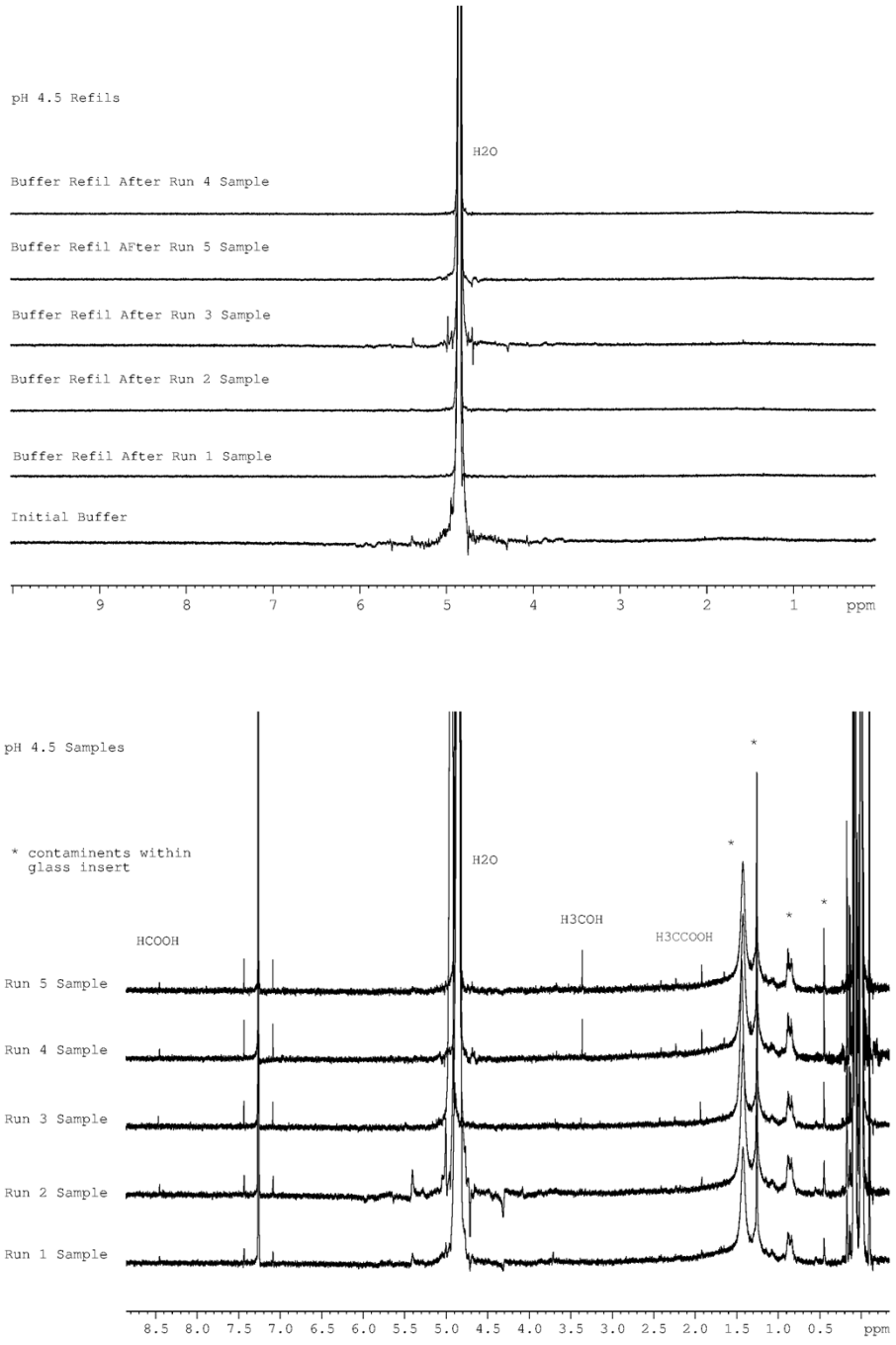

Figure S18- ^{1}H NMR spectra showing top, PBS refills showing no contamination present, bottom, sample taken during catalysis.

pH 6.5

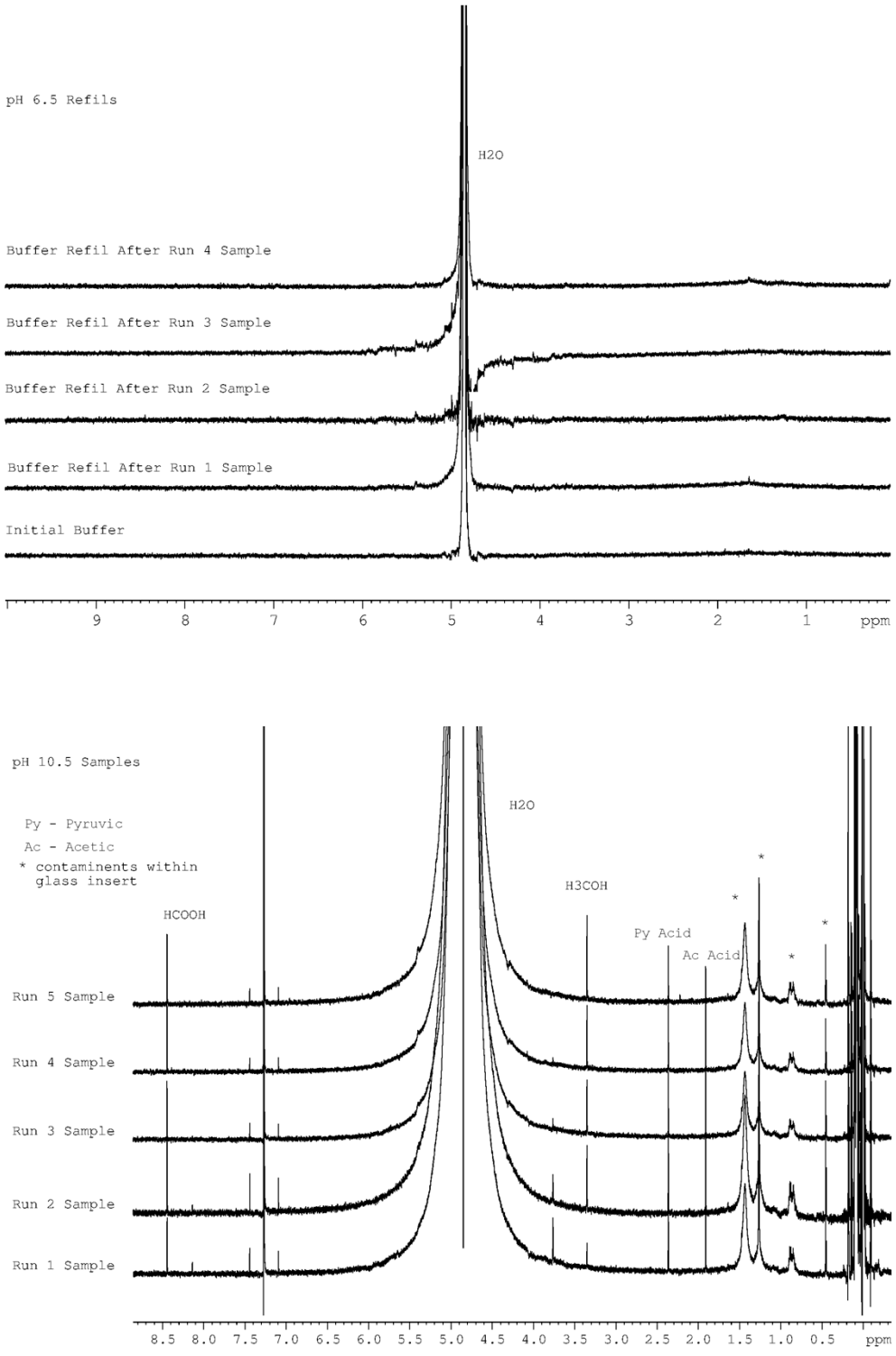

Figure S19- ^{1}H NMR spectra showing top, PBS refills showing no contamination present, bottom, sample taken during catalysis.

pH 10.5

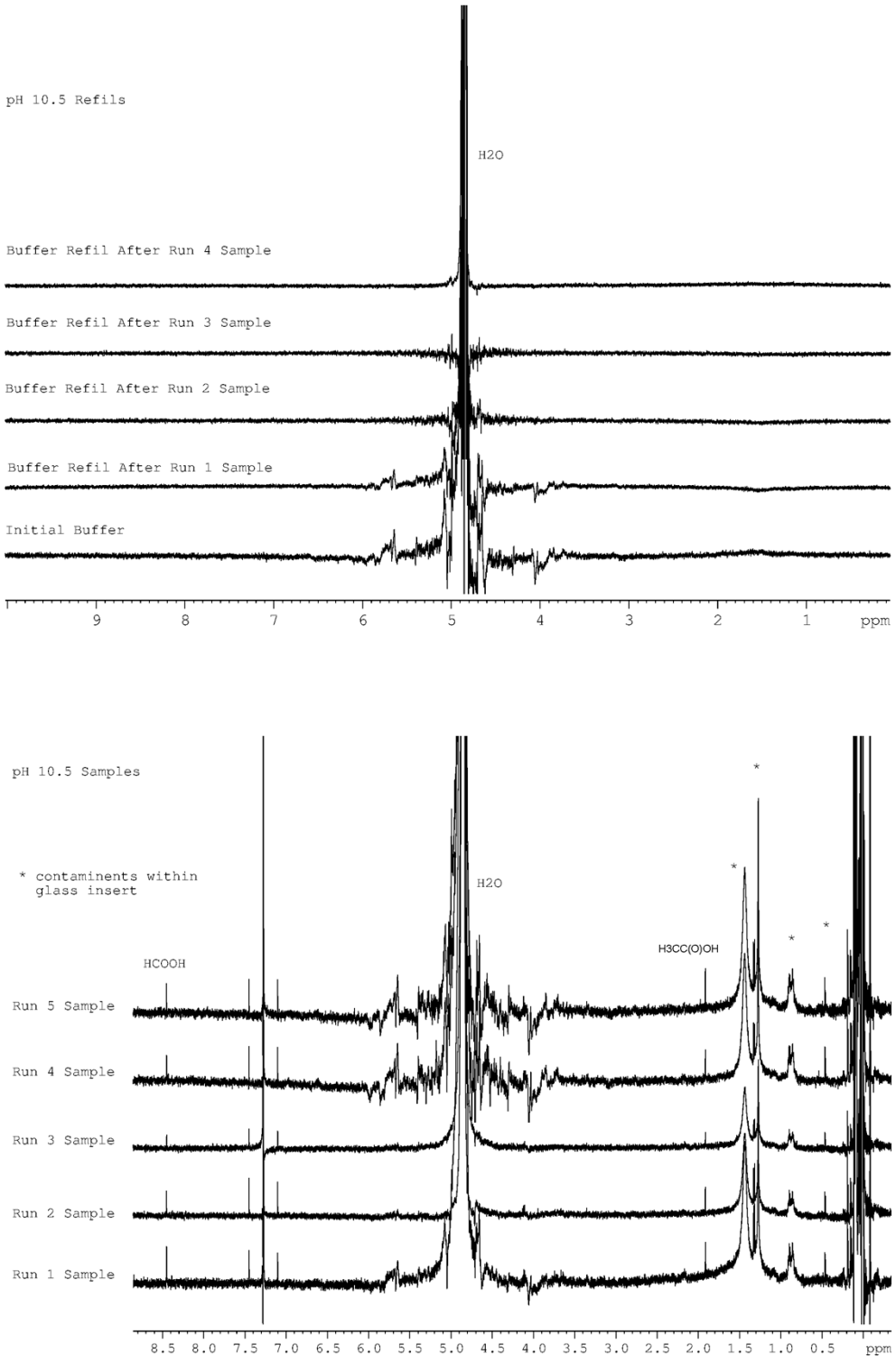

Figure S20- ^{1}H NMR spectra showing top, PBS refills showing no contamination present, bottom, sample taken during catalysis.

S3.5.2 Cumulative data tables

Table S2 – Total product detected by ^{1}H NMR at pH 4.5

pH 4.5	No of scans (0 to -1V to 0V)	Formic Acid (umols)	Methanol (umols)	Pyruvic Acid (umols)	Acetic Acid (umols)
Sample 1	45	0.0268	0.0202	0.0000	0.0101
Sample 2	83	0.0528	0.0202	0.0000	0.0242
Sample 3	127	0.0785	0.0202	0.0000	0.0397
Sample 4	171	0.0987	0.0486	0.0000	0.0537
Sample 5	211	0.1181	0.0800	0.0000	0.0663

Table S3 - Total product detected by ^{1}H NMR at pH 6.5

pH 6.5	No of scans (0 to -1V to 0V)	Formic Acid (umols)	Methanol (umols)	Pyruvic Acid (umols)	Acetic Acid (umols)
Sample 1	42	0.2486	0.0287	0.1147	0.1210
Sample 2	84	0.5122	0.0926	0.2194	0.2361
Sample 3	123	0.7888	0.1737	0.3249	0.3539
Sample 4	168	1.0754	0.2622	0.4256	0.4632
Sample 5	217	1.3271	0.3546	0.4892	0.5724

Table S4 - Total product detected by ^{1}H NMR at pH 10.5

pH 10.5	No of scans (0 to -1V to 0V)	Formic Acid (umols)	Methanol (umols)	Pyruvic Acid (umols)	Acetic Acid (umols)
Sample 1	43	0.1421	0.0000	0.0000	0.0357
Sample 2	85	0.2206	0.0000	0.0000	0.0634
Sample 3	125	0.2933	0.0000	0.0000	0.0897
Sample 4	169	0.3713	0.0000	0.0000	0.1182
Sample 5	213	0.4272	0.0000	0.0000	0.1447

S3.5.3 Electrochemistry

The CVs displayed below are from the first *ca.* 40 cycles prior to the first sample. Only the first 40 scans are shown, these are representative of the features seen during potential cycling over the remaining scans.

pH 4.5

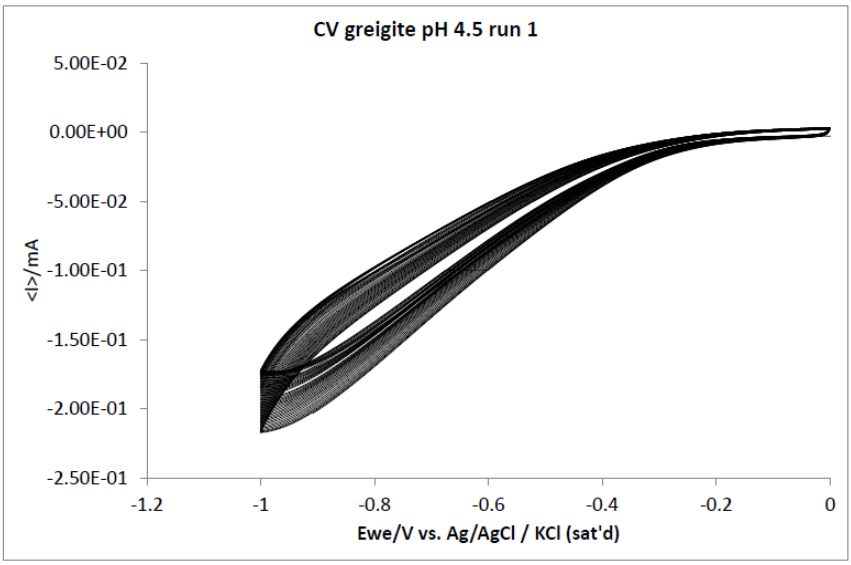

pH 6.5

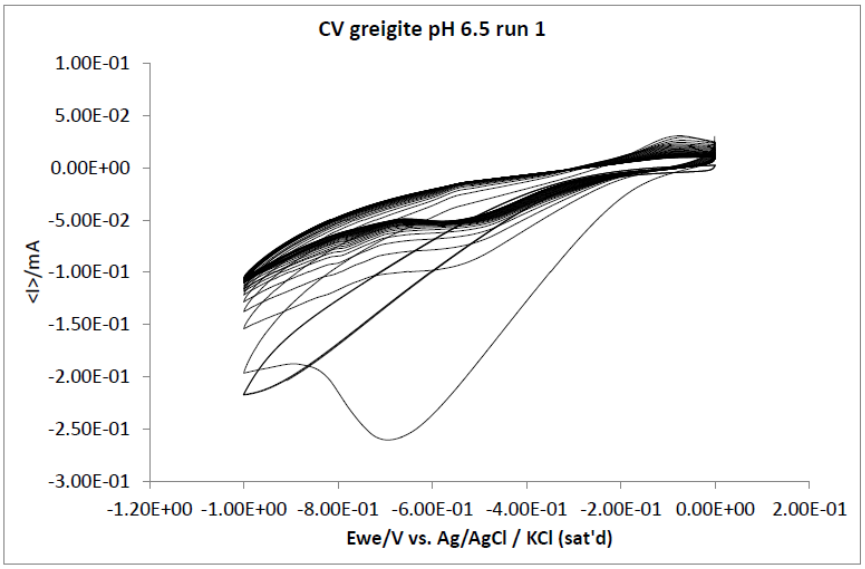

pH 10.5

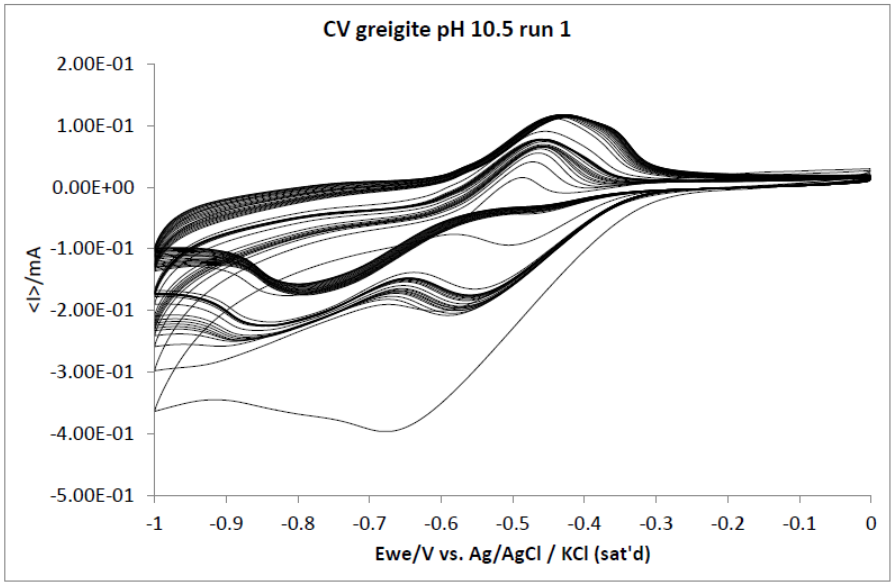

S3.5.4 Efficiency

Faradaic efficiencies have been calculated assuming;

Formic Acid = 2 electron reduction

$CO_2 + 2\ H^+ + 2\ e^- \rightarrow \mathbf{HCO_2H}$

Methanol = 6 electron reduction

$CO_2 + 6\ H^+ + 6\ e^- \rightarrow \mathbf{CH_3OH} + H_2O$

Acetic Acid = 8 electron reduction

$CO_2 + 2\ H^+ + 2\ e^- \rightarrow HCO_2H$
$CO_2 + 6\ H^+ + 6\ e^- \rightarrow CH_3OH + H_2O$
$HCO_2H + CH_3OH \rightarrow \mathbf{CH_3CO_2H} + H_2O$ (dehydration)

Pyruvic acid = 10 electron reduction

$2CO_2 + 4\ H^+ + 4\ e^- \rightarrow 2HCO_2H$
$CO_2 + 6\ H^+ + 6\ e^- \rightarrow CH_3OH + H_2O$
$HCO_2H + CH_3OH \rightarrow CH_3CO_2H + H_2O$ (dehydration)
$CH_3CO_2H + HCO_2H \rightarrow \mathbf{CH_3COCOOH} + H_2O$ (dehydration)

pH	Total charge passed (Coulombs)	Faraday efficiency (%)				
		Formic Acid	Methanol	Acetic Acid	Pyruvic Acid	Total
4.5	22.42	0.1	0.21	0.23	-	0.54
6.5	16.96	1.51	1.21	2.61	2.78	8.11
10.5	22.43	0.37	-	0.5	-	0.87

The charge passed has been processed from integrating the CV data using the process data function within EC-lab V10.10.

S3.5.5 Potential Hold Study

An identical setup and cleaning procedures explained in S1.2 was performed the exception being the applied potential was held at a fixed potential and then an ^{1}H NMR taken to determine the onset of product formation. Each new potential is a separate experiment and a new WE and electrolyte was used.

Potential Held at (V)	Formic acid peak seen
0.0	No
-0.2	No
-0.4	Yes
-0.6	Yes

The signal to noise ratio for experiments where formic acid was detected is too low for reliable quantification, although a suitable for qualitative assessment.

3.6 Computational model

S3.6.1 Slab model

The Fe_3S_4 surfaces were prepared by cutting the bulk structure using the METADISE code[17] and creating a slab model. This code not only considers periodicity on the plane direction but also provides the different stacking atomic layer resulting in a null dipole moment perpendicular to the surface plane.[18] We considered the most stable termination for both {001} and {111} surfaces with a respective surface area of 81.0 and 93.5 $Å^2$. The slabs contain 56 atoms (24 Fe and 32 S) per unit cell and we added a vacuum width of 12 Å between periodic slabs, i.e. big enough to avoid perpendicular interaction. The slabs are also thick enough to relax the two uppermost layers (four Fe_3S_4 units) until energy convergence, keeping the bulk structure frozen at the bottom. Isolated adsorbate molecules were placed in the centre of a 15x15x15 $Å^3$ simulation cell, avoiding lateral interactions and using the same criteria of convergence as for the surface slabs.

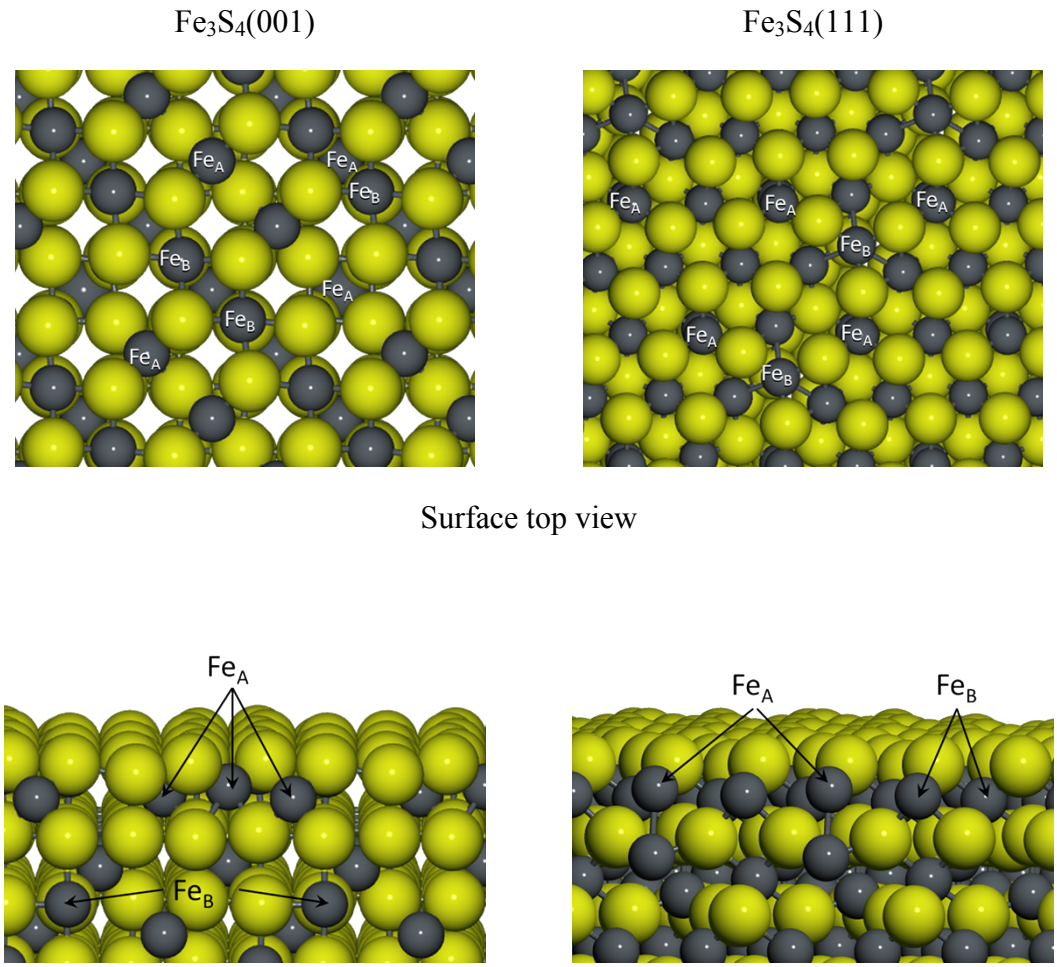

Figure S21- Representation of geometry-optimised (001) and (111) slabs of Fe_3S_4, where the Fe_A and Fe_B are indicated in the surface. Colour scheme: grey shows Fe atoms, yellow is S, light-grey is C and red indicate O atoms

S3.6.2 Slab model

The Fe_3S_4 surfaces were prepared by cutting the bulk structure using the METADISE

S6.6.3 Multiple Pathways

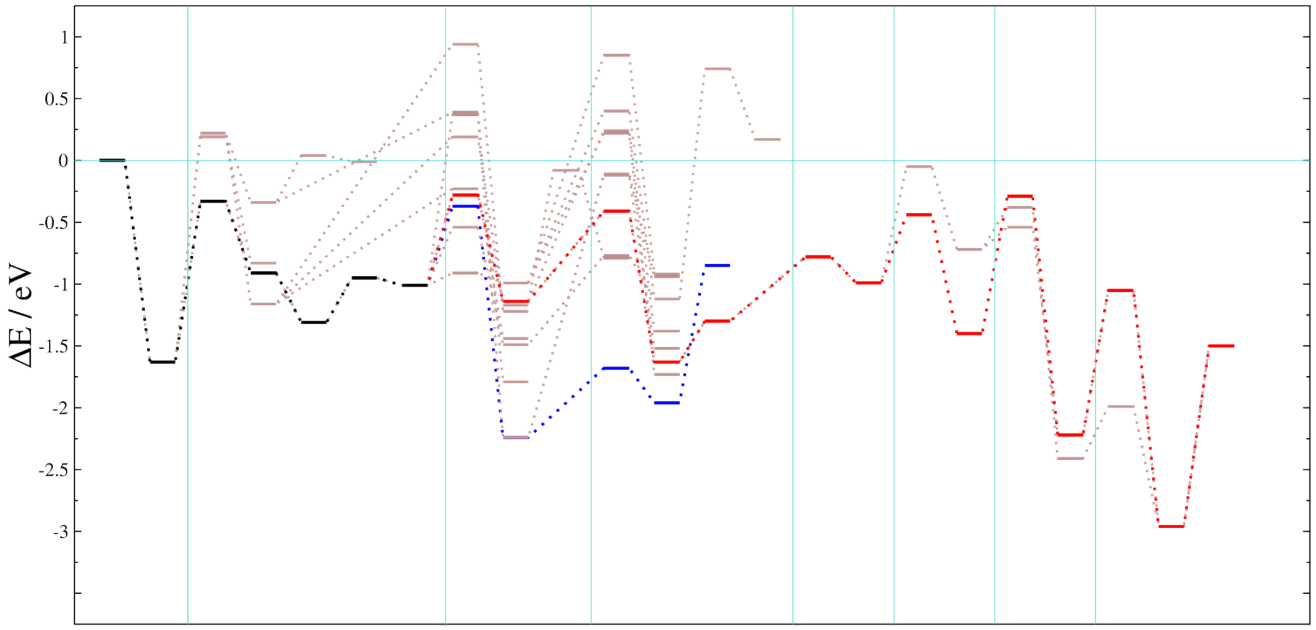

Figure S23- Energetic profile of the multiple pathways for the transformation of HCO_3^- on the Fe_3S_4(111) slab. Bold colour lines show the pathways leading to HCOOH (blue) and CH_3OH (red) molecules.